Kalman Filter State Transformation Application in INS/GNSS Integrated Navigation for Polar Navigation

Honggang Guo, Zhikun Liao, Zhonghong Liang, Pengcheng Mu, Jie Yuan, Lin Wang
College of Advanced Interdisciplinary Studies, National University of Defense Technology, Changsha, China
Nanhu Laser Laboratory National University of Defense Technology, Changsha, China
guohonggang2021@163.com, lzkun2008@yeah.net, lzhgzyx1@163.com, pengcheng_1997@163.com, jieyuan@nudt.edu.cn, wanglin11@nudt.edu.cn

***Abstract*—Kalman filter is an important technology to realize information fusion between Inertial Navigation System (INS) and Global Navigation Satellite System (GNSS). One of the most important variables in the Kalman filter structure is the state variable, which is the basis of maintaining system stability. However, due to the inherent singularity in polar regions, the INS/GNSS integrated navigation system will not work properly in polar regions. Different coordinate systems are often used in trans-polar navigation to solve the problems in the polar regions, therefore the Kalman filter state variable transformation is inevitable in the process of entering or leaving the polar regions, which will bring instability and even failure to the system. Here, this paper proposes a Kalman filter state transformation algorithm for INS/GNSS polar integrated navigation based on Psi-angle error model to ensure the numerical stability of the Kalman filter during its state transformation. Key to this success is to establish the transformation relationship between different filter state variables as well as their covariance matrices in different navigation coordinate systems, then the state variables and the covariance matrices are transformed simultaneously. After presenting the state variable transformation algorithm and the system description, a numerical evaluation is carried out to assess the presented algorithm with regard to stability and accuracy.**

Keywords—Kalman filter, state variables transformation, INS/GNSS Integrated Navigation, polar Navigation

I. INTRODUCTION

Integrated navigation system is one of typical application of Kalman filter to realize information fusion. In the past few decades, many research efforts have been devoted to developing the information fusion between different sensors and Inertial Navigation System (INS) to solve the inevitable error divergence problem in pure inertial navigation, forming different integrated navigation modes [1], [2]. Since INS is an integral calculation process, its errors accumulate and diverge with time, while the position information provided by GNSS does not diverge with time. In addition, INS can provide short-time high-precision positioning results under the failure or interference of GNSS. Due to its excellent complementary characteristics, the Global Navigation Satellite System (GNSS)-aided INS integrated navigation system, designed by Kalman filter, has become an important navigation method in the maritime navigation [3].

The polar navigation is a significant research area of INS/GNSS integrated navigation. Due to the special geographical location of the polar regions, GNSS is easily affected by the polar electromagnetic environment or even loses signals [4]. To overcome the effects of the environment on the system, researchers focus on some adaptive filtering methods to improve robustness of INS/GNSS integrated navigation system or build a more elaborate integrated navigation system model to estimate and compensate the system states. [5], [6]. However, the transformation of state variables is easily ignored. As an indispensable and important variable in Kalman filter structure, state variables have an important impact on the stability of INS/GNSS integrated navigation system. Fu et al. [7] pointed that when the state space change, its covariance matrix changes concurrently, which destroys the original stable gain of the system and causes discontinuity of the system, then, Kalman filter enters a short unstable period. In fact, the navigation coordinate system switching and the Kalman filter state variables transformation are inevitable in the process of a carrier entering or leaving the polar regions. This is because that with the rapid increase of latitude near the polar regions, the traditional navigation algorithm of inertial navigation appears computation overflow near the pole and singularity at the pole, it is no longer suitable for the polar region navigation. To address the issue, a lot of the polar navigation work focus on the two schemes of transversal mechanism and grid mechanism, in which the INS/GNSS integrated navigation system can work well [7]-[11].Therefore, in order to ensure that the navigation information provided by INS/GNSS integrated navigation system is reliable and effective, it must involve the problem of the Kalman filter state variable transformation between different coordinate systems .

In order to solve the problem of filter discontinuity caused by Kalman filter state variables transformation. Zhang et al. [12] designed a transformation algorithm to handle this problem, which ensures that the state variables and its covariance matrix can be switched synchronously during the navigation coordinate system switching process. In his study, the sate variables transformation relationship between the grid and the local-level geographic coordinate system is derived, which reduces the oscillation error caused by navigation coordinate system switching. However, the complicated expressions of the approach bring trouble to the navigation solution. Inspired by this study, on the basis of the Psi-angle error model, this paper derives the sate variables transformation relationship between the transversal and the local-level geographic coordinate system mechanization. Not only is the Psi-angle defined in a known coordinate system, the perturbation error related with the true navigation coordinate system is absent, but also it can better fuse with GNSS measurement data and modify the INS [13]-[15]. Therefore, this paper proposes a state variables transformation algorithm based on Psi-angle error model, which greatly

XXX-X-XXXX-XXXX-X/XX/$XX.00 ©20XX IEEE

simplifies the transformation matrix, reduces the approximate error, and brings convenience to the navigation solution.

One of the contribution of this paper, a more concise Kalman filter state transformation algorithm is proposed for INS/GNSS polar integrated navigation system. In addition, the open loop mode and closed loop mode are two different feedback modes of Kalman filter, and they have different characteristics in INS/GNSS integrated navigation. Therefore, another contribution of this paper is to discuss the different effects of the proposed algorithm on INS/GNSS integrated navigation systems with open loop mode and closed loop mode. The remainder of the paper is organized as follows. In section II, the dynamical model and observation model of INS/GNSS integrated navigation system are established based on the Psi-angle error model. Section III systematically deduces the transformation relation of error state and its covariance matrix. Section IV verifies the effectiveness of the proposed algorithm and analyzes the influence of the proposed algorithm on the system under different feedback methods, and the conclusion is presented in Section V.

II. INS/GNSS Integrated Navigation System Model

Typically, there are two types of models to describe the INS error state: the Psi-angle error model and the Phi-angle error model. These models have slight differences in their projected coordinate systems, but they are essentially equivalent [16]. The Psi-angle error model, which projects the system error state onto a known computational navigation frame, can reduce system complexity and computational load to some extent. Therefore, this paper adopts the Psi-angle error model to describe the dynamics of the system.

A. Dynamic Model

The dynamic model of INS/GNSS integrated navigation can be expressed as

$$\dot{\mathbf{X}} = \mathbf{F}\mathbf{X} + \mathbf{G}\mathbf{w} \tag{1}$$

where $\mathbf{F}$ represents the state transition matrix; $\mathbf{G}$ represents the system distribution noise matrix; $\mathbf{w}$ represents system noise vector; $\mathbf{X}$ represents the error state vector, as (2) shows

$$\mathbf{X} = [(\boldsymbol{\psi}^{\mathrm{n}})^{\mathrm{T}} \ (\delta\mathbf{v}^{\mathrm{n}})^{\mathrm{T}} \ (\delta\mathbf{r}^{\mathrm{n}})^{\mathrm{T}} \ (\boldsymbol{\varepsilon}^{\mathrm{b}})^{\mathrm{T}} \ (\boldsymbol{\nabla}^{\mathrm{b}})^{\mathrm{T}} \ (\delta\boldsymbol{l}^{\mathrm{b}})^{\mathrm{T}}]^{\mathrm{T}} \tag{2}$$

where n denotes the navigation frame, specifically speaking, the navigation frame refers to the computational geographic coordinate system in non-polar regions or the computational transversal geographic coordinate system in polar regions; b denotes the body frame; $\boldsymbol{\psi}^{\mathrm{n}}=[\psi_{\mathrm{E}}^{\mathrm{n}} \ \psi_{\mathrm{N}}^{\mathrm{n}} \ \psi_{\mathrm{U}}^{\mathrm{n}}]^{\mathrm{T}}$ is the drift error angle, referring to the error between the computational coordinate system, in the n-frame; $\delta\mathbf{v}^{\mathrm{n}}=[\delta v_{\mathrm{E}}^{\mathrm{n}} \ \delta v_{\mathrm{N}}^{\mathrm{n}} \ \delta v_{\mathrm{U}}^{\mathrm{n}}]^{\mathrm{T}}$ is the velocity error in the n-frame; $\delta\mathbf{r}^{\mathrm{n}}=[\delta r_{\mathrm{E}}^{\mathrm{n}} \ \delta r_{\mathrm{N}}^{\mathrm{n}} \ \delta r_{\mathrm{U}}^{\mathrm{n}}]^{\mathrm{T}}$ is the position error in the n-frame; $\boldsymbol{\varepsilon}^{\mathrm{b}}=[\varepsilon_{x}^{\mathrm{b}} \ \varepsilon_{y}^{\mathrm{b}} \ \varepsilon_{z}^{\mathrm{b}}]^{\mathrm{T}}$ and $\boldsymbol{\nabla}^{\mathrm{b}}=[\nabla_{x}^{\mathrm{b}} \ \nabla_{y}^{\mathrm{b}} \ \nabla_{z}^{\mathrm{b}}]^{\mathrm{T}}$ are the gyro and accelerometer drift bias in the b-frame; $\delta\boldsymbol{l}^{\mathrm{b}}=[\delta l_{x}^{\mathrm{b}} \ \delta l_{y}^{\mathrm{b}} \ \delta l_{z}^{\mathrm{b}}]^{\mathrm{T}}$ is the lever arm error between the INS and the GNSS antenna in the b-frame.

The INS error equations are introduced to describe the concrete dynamic of (1), and the error equations for the drift error angle, the velocity error and the position error can be described as

$$\dot{\boldsymbol{\psi}}^{\mathrm{n}} = -(\boldsymbol{\omega}_{\mathrm{ie}}^{\mathrm{n}} + \boldsymbol{\omega}_{\mathrm{en}}^{\mathrm{n}}) \times \boldsymbol{\psi}^{\mathrm{n}} - \mathbf{C}_{\mathrm{b}}^{\mathrm{n}}\delta\boldsymbol{\omega}_{\mathrm{ib}}^{\mathrm{b}} \tag{3}$$

$$\delta\dot{\mathbf{v}}^{\mathrm{n}} = (\mathbf{C}_{\mathrm{b}}^{\mathrm{n}}\mathbf{f}^{\mathrm{b}}) \times \boldsymbol{\psi}^{\mathrm{n}} - (2\boldsymbol{\omega}_{\mathrm{ie}}^{\mathrm{n}} + \boldsymbol{\omega}_{\mathrm{en}}^{\mathrm{n}}) \times \delta\mathbf{v}^{\mathrm{n}} + \mathbf{C}_{\mathrm{b}}^{\mathrm{n}}\delta\mathbf{f}_{\mathrm{ib}}^{\mathrm{b}} \tag{4}$$

$$\delta\dot{\mathbf{r}}^{\mathrm{n}} = -\boldsymbol{\omega}_{\mathrm{en}}^{\mathrm{n}} \times \delta\mathbf{r}^{\mathrm{n}} + \delta\mathbf{v}^{\mathrm{n}} \tag{5}$$

where i denotes the inertial frame; e denotes the Earth-centered Earth-fixed fame; $\boldsymbol{\omega}_{\mathrm{ie}}^{\mathrm{n}}$ represents the earth rotation angle velocity vector in the n-frame; $\boldsymbol{\omega}_{\mathrm{en}}^{\mathrm{n}}$ represents the rotating angle velocity vector of the n-frame relative to the e-frame in the n-frame; $\mathbf{C}_{\mathrm{b}}^{\mathrm{n}}$ represents the direction cosine matrix from the b-frame to n-frame; $\delta\boldsymbol{\omega}_{\mathrm{ib}}^{\mathrm{b}}$ represents the measurement error of the gyroscope; $\mathbf{f}^{\mathrm{b}}$ represents the specific force measured by accelerometers in the body frame, whose error is $\delta\mathbf{f}_{\mathrm{ib}}^{\mathrm{b}}$; $\delta\boldsymbol{\omega}_{\mathrm{ib}}^{\mathrm{b}}$ and $\delta\mathbf{f}_{\mathrm{ib}}^{\mathrm{b}}$ are given by

$$\delta\boldsymbol{\omega}_{\mathrm{ib}}^{\mathrm{b}} = \boldsymbol{\varepsilon}^{\mathrm{b}} + \mathbf{w}_{\mathrm{g}}^{\mathrm{b}} \tag{6}$$

$$\delta\mathbf{f}_{\mathrm{ib}}^{\mathrm{b}} = \nabla^{\mathrm{b}} + \mathbf{w}_{\mathrm{a}}^{\mathrm{b}} \tag{7}$$

where $\mathbf{w}_{\mathrm{g}}^{\mathrm{b}}$ and $\mathbf{w}_{\mathrm{a}}^{\mathrm{b}}$ are the Gaussian white noise of gyro and accelerometer respectively; the gyro drift bias $\boldsymbol{\varepsilon}^{\mathrm{b}}$ and the accelerometer drift bias ∇^{b} can be described by the first-order Markov process errors, which are shown by

$$\dot{\boldsymbol{\varepsilon}}^{\mathrm{b}} = -\boldsymbol{\varepsilon}^{\mathrm{b}}/\boldsymbol{\tau}_{\varepsilon} + \mathbf{w}_{\varepsilon} \tag{8}$$

$$\dot{\boldsymbol{\nabla}}^{\mathrm{b}} = -\boldsymbol{\nabla}^{\mathrm{b}}/\boldsymbol{\tau}_{\nabla} + \mathbf{w}_{\nabla} \tag{9}$$

where $\boldsymbol{\tau}_{\varepsilon}$ and $\boldsymbol{\tau}_{\nabla}$ are the Markov correlation time of the gyro and accelerometer respectively; $\mathbf{w}_{\varepsilon}$ and $\mathbf{w}_{\nabla}$ represent the driving white noise of the gyro and accelerometer respectively. The lever arm can be regarded as rigid, and the differential equation of the lever arm error can be written as

$$\delta\dot{\boldsymbol{l}}^{\mathrm{b}} = 0 \tag{10}$$

According to the above differential equations, the specific form of the system dynamic model can be written.

B. Measurement Model

The measurement model of INS/GNSS integrated navigation can be expressed as

$$\mathbf{Z} = \mathbf{H}\mathbf{X} + \boldsymbol{\upsilon} \tag{11}$$

where $\mathbf{Z}$ represents system measurement vector; $\mathbf{H}$ represents system measurement matrix; $\boldsymbol{\upsilon}$ represents system measurement white noise. Due to the presence of the lever arm, the position relationship between the INS and the GNSS antenna in e-frame or n-frame can be expressed as

$$\mathbf{r}_{\mathrm{GNSS}}^{\mathrm{e}} = \mathbf{r}_{\mathrm{INS}}^{\mathrm{e}} + \mathbf{C}_{\mathrm{b}}^{\mathrm{e}}\boldsymbol{l}^{\mathrm{b}} \tag{12}$$

$$\mathbf{r}_{\mathrm{GNSS}}^{\mathrm{n}} = \mathbf{r}_{\mathrm{INS}}^{\mathrm{n}} + \mathbf{C}_{\mathrm{b}}^{\mathrm{n}}\boldsymbol{l}^{\mathrm{b}} \tag{13}$$

where $\mathbf{r}^{e}$ is the carrier position vector in the e-frame, which means the radius vector between the carrier and the center of the earth, and $\mathbf{r}^{n}$ is the carrier position vector in the n-frame; The subscript indicates that the data comes from GNSS or INS, $\mathbf{C}_{b}^{e}$ represents the direction cosine matrix from the b-frame to e-frame; $\boldsymbol{l}^{b}$ is the lever arm, which can be written as

$$\boldsymbol{l}^{b} = \boldsymbol{l}_{0}^{b} + \delta\boldsymbol{l}^{b} \tag{14}$$

where $\boldsymbol{l}_{0}^{b}$ is the initial lever arm; When the GNSS position information is used as observation, after compensating for the lever arm error through (12) the system measurement vector $\mathbf{Z}$ can be expressed as

$$\mathbf{Z} = \mathbf{C}_{e}^{n}\tilde{\mathbf{r}}_{INS}^{e} + \mathbf{C}_{e}^{n}\tilde{\mathbf{C}}_{b}^{e}\boldsymbol{l}^{b} - \mathbf{C}_{e}^{n}\tilde{\mathbf{r}}_{GNSS}^{e} \tag{15}$$

where superscript $\tilde{\bullet}$ represents the vector $\bullet$ with error; the $\tilde{\mathbf{r}}_{INS}^{n}$ and $\tilde{\mathbf{r}}_{GNSS}^{n}$ are the position information with measurement error from INS and GNSS; Since the n-frame is the computational coordinate system, which is a known coordinate system, there is no error in the direction cosine matrix $\mathbf{C}_{e}^{n}$. Moreover, the direction cosine matrix $\tilde{\mathbf{C}}_{b}^{e}$ can be expressed as

$$\tilde{\mathbf{C}}_{b}^{e} = (\mathbf{I} - [\boldsymbol{\psi}^{e}\times])\mathbf{C}_{b}^{e} \tag{16}$$

where

$$[\mathbf{a}\times] = \begin{bmatrix} 0 & -\mathbf{a}_{z} & \mathbf{a}_{y} \\ \mathbf{a}_{z} & 0 & -\mathbf{a}_{x} \\ -\mathbf{a}_{y} & \mathbf{a}_{x} & 0 \end{bmatrix} \tag{17}$$

substituting (16) into (15) and rearranging it, the system measurement vector $\mathbf{Z}$ can be rewritten as

$$\mathbf{Z} = [(\mathbf{C}_{b}^{n}\boldsymbol{l}_{0}^{b})\times]\boldsymbol{\psi}^{n} + \delta\mathbf{r}^{n} + \mathbf{C}_{b}^{n}\delta\boldsymbol{l}^{b} + \boldsymbol{\upsilon} \tag{18}$$

III. KALMAN FILTER STATE TRANSFORMATION

When the INS mechanization is performed at different coordinate systems, the filter states are also different. Taking the carrier entering the polar region as an example, the filter states of the navigation coordinate system will undergo a transition. When the INS works at mid to low latitudes, the state equation of the Kalman filter system is described as

$$\dot{\mathbf{X}}^{c} = \mathbf{F}_{1}\mathbf{X}^{c} + \mathbf{G}_{1}\mathbf{w} \tag{19}$$

where c denotes computational geographic coordinate system; When the INS works in the polar regions, the state equation of the Kalman filter system is

$$\dot{\mathbf{X}}^{c'} = \mathbf{F}_{2}\mathbf{X}^{c'} + \mathbf{G}_{2}\mathbf{w} \tag{20}$$

where c' denotes the computational transversal geographic coordinate system; It should be noted that the c and c' here is a specific representation of the navigation coordinate system n. The definition relating to the transversal system is described in detail in [8]. In this section, by using the true coordinate system as a bridge, the relationship between different filter state variables in the computational coordinate system can be established based on perturbation method, achieving smooth switching of Kalman filter structure [14], [17], [18].

Firstly, start with the Phi-angle error model, the transformation relationship between the drift error angle $\boldsymbol{\psi}^{c}$ and $\boldsymbol{\psi}^{c'}$ will be derived. By using the chain rule of the direction cosine matrix, the direction cosine matrix $\mathbf{C}_{b}^{t}$ can be written as

$$\mathbf{C}_{b}^{t} = \mathbf{C}_{g}^{t}\mathbf{C}_{b}^{g} \tag{21}$$

where g denotes the true geographic coordinate system; t denotes the true transversal geographic coordinate system. Perturbation of (21) is

$$\delta\mathbf{C}_{b}^{t} = \delta\mathbf{C}_{g}^{t}\mathbf{C}_{b}^{g} + \mathbf{C}_{g}^{t}\delta\mathbf{C}_{b}^{g} \tag{22}$$

Similarly, perturbation of the direction cosine matrix $\delta\mathbf{C}_{g}^{t}$ is

$$\delta\mathbf{C}_{g}^{t} = \delta(\mathbf{C}_{e}^{t}\mathbf{C}_{g}^{e}) = \delta\mathbf{C}_{e}^{t}\mathbf{C}_{g}^{e} + \mathbf{C}_{e}^{t}\delta\mathbf{C}_{g}^{e} \tag{23}$$

some basic equation can be found in the literature [14],[17], as shown

$$\begin{cases} \delta\mathbf{C}_{b}^{t} = -[\boldsymbol{\phi}^{t}\times]\mathbf{C}_{b}^{t}, & \delta\mathbf{C}_{b}^{g} = -[\boldsymbol{\phi}^{g}\times]\mathbf{C}_{b}^{g} \\ \delta\mathbf{C}_{e}^{t} = -[\delta\boldsymbol{\theta}^{t}\times]\mathbf{C}_{e}^{t}, & \delta\mathbf{C}_{e}^{g} = -[\delta\boldsymbol{\theta}^{g}\times]\mathbf{C}_{e}^{g} \end{cases} \tag{24}$$

where $\boldsymbol{\phi}^{t}$ and $\boldsymbol{\phi}^{g}$ is attitude error angle in the t-frame and the g-frame; $\delta\boldsymbol{\theta}^{t}$ and $\delta\boldsymbol{\theta}^{g}$ is position error angle in the t-frame and the g-frame; Substituting (23) and (24) into (22) yields

$$\boldsymbol{\phi}^{t} - \delta\boldsymbol{\theta}^{t} = \mathbf{C}_{g}^{t}(\boldsymbol{\phi}^{g} - \delta\boldsymbol{\theta}^{g}) \tag{25}$$

moreover, the relationship between attitude error angle $\boldsymbol{\phi}$, position error angle $\delta\boldsymbol{\theta}$ and drift error angle $\boldsymbol{\psi}$ is

$$\boldsymbol{\phi} = \boldsymbol{\psi} + \delta\boldsymbol{\theta} \tag{26}$$

thus, (25) can be rewritten as

$$\boldsymbol{\psi}^{t} = \mathbf{C}_{g}^{t}\boldsymbol{\psi}^{g} \tag{27}$$

Furthermore, by using the chain rule of the direction cosine matrix $\boldsymbol{\psi}^{g} = \mathbf{C}_{c}^{g}\boldsymbol{\psi}^{c}$ and $\boldsymbol{\psi}^{t} = \mathbf{C}_{c'}^{t}\boldsymbol{\psi}^{c'}$, the transformation relationship between the drift error angle $\boldsymbol{\psi}^{c}$ and $\boldsymbol{\psi}^{c'}$ can be obtained as

$$\boldsymbol{\psi}^{c'} = \mathbf{C}_{c}^{c'}\boldsymbol{\psi}^{c} \tag{28}$$

Secondly, the velocity relationship in the g-frame and t-frame can be written as

$$\mathbf{v}^{t} = \mathbf{C}_{g}^{t}\mathbf{v}^{g} \tag{29}$$

perturbation of the (29) is

$$\delta \mathbf{v}^{\mathrm{t}} = \delta \mathbf{C}_{\mathrm{g}}^{\mathrm{t}} \mathbf{v}^{\mathrm{g}} + \mathbf{C}_{\mathrm{g}}^{\mathrm{t}} \delta \mathbf{v}^{\mathrm{g}} \tag{30}$$

substituting (23) and (24) into (30) yields

$$\delta \mathbf{v}^{\mathrm{t}} + [\delta \boldsymbol{\theta}^{\mathrm{t}} \times] \mathbf{v}^{\mathrm{t}} = \mathbf{C}_{\mathrm{g}}^{\mathrm{t}} ([\delta \boldsymbol{\theta}^{\mathrm{g}} \times] \mathbf{v}^{\mathrm{g}} + \delta \mathbf{v}^{\mathrm{g}}) \tag{31}$$

Moreover, the relationship between the velocity error in the true coordinate system and the computational coordinate system is

$$\delta \mathbf{v}^{\mathrm{t}} + [\delta \boldsymbol{\theta}^{\mathrm{t}} \times] \mathbf{v}^{\mathrm{t}} = \delta \mathbf{v}^{\mathrm{c}'}, \quad \delta \mathbf{v}^{\mathrm{g}} + [\delta \boldsymbol{\theta}^{\mathrm{g}} \times] \mathbf{v}^{\mathrm{g}} = \delta \mathbf{v}^{\mathrm{c}} \tag{32}$$

substituting (32) into (31), the transformation relationship between velocity error $\delta \mathbf{v}^{\mathrm{c}}$ and $\delta \mathbf{v}^{\mathrm{c}'}$ can be obtained as

$$\delta \mathbf{v}^{\mathrm{c}'} = \mathbf{C}_{\mathrm{g}}^{\mathrm{t}} \delta \mathbf{v}^{\mathrm{c}} \tag{33}$$

with $\mathbf{C}_{\mathrm{g}}^{\mathrm{t}} = \mathbf{C}_{\mathrm{c}'}^{\mathrm{t}} \mathbf{C}_{\mathrm{c}}^{\mathrm{c}'} \mathbf{C}_{\mathrm{g}}^{\mathrm{c}}$, $\mathbf{C}_{\mathrm{c}'}^{\mathrm{t}}$ and $\mathbf{C}_{\mathrm{g}}^{\mathrm{c}}$ can be found in the literature [17], as shown

$$\mathbf{C}_{\mathrm{g}}^{\mathrm{c}} = \mathbf{I} - [\delta \boldsymbol{\theta}^{\mathrm{g}} \times], \quad \mathbf{C}_{\mathrm{c}'}^{\mathrm{t}} = \mathbf{I} + [\delta \boldsymbol{\theta}^{\mathrm{t}} \times] \tag{34}$$

ignoring the second order small quantity can get the equation $\mathbf{C}_{\mathrm{c}}^{\mathrm{c}'} \approx \mathbf{C}_{\mathrm{g}}^{\mathrm{t}}$; Thus, the transformation relationship between velocity error $\delta \mathbf{v}^{\mathrm{c}}$ and $\delta \mathbf{v}^{\mathrm{c}'}$ can be obtained as:

$$\delta \mathbf{v}^{\mathrm{c}'} = \mathbf{C}_{\mathrm{c}}^{\mathrm{c}'} \delta \mathbf{v}^{\mathrm{c}} \tag{35}$$

In the same way as the velocity error transformation, the transformation relationship between position error $\delta \mathbf{r}^{\mathrm{c}}$ and $\delta \mathbf{r}^{\mathrm{c}'}$ can be obtained as

$$\delta \mathbf{r}^{\mathrm{c}'} = \mathbf{C}_{\mathrm{c}}^{\mathrm{c}'} \delta \mathbf{r}^{\mathrm{c}} \tag{36}$$

In this paper, the drift angle error, the velocity error and the position error of Kalman filter need to be transformed when their projection coordinate system undergoes transformation. The projection coordinate system of the remaining states, i.e., the gyro drift, accelerometer bias and the lever arm error are in the b-frame, which does not change, so there is no need for transformation. The transformation relationship of state variables between $\mathbf{X}^{\mathrm{c}}$ and $\mathbf{X}^{\mathrm{c}'}$ can be expressed in matrix form as

$$\mathbf{X}^{\mathrm{c}'} = \boldsymbol{\Phi} \mathbf{X}^{\mathrm{c}} \tag{37}$$

where $\boldsymbol{\Phi} = \mathrm{diag}\left\{\mathbf{C}_{\mathrm{c}}^{\mathrm{c}'} \quad \mathbf{C}_{\mathrm{c}}^{\mathrm{c}'} \quad \mathbf{C}_{\mathrm{c}}^{\mathrm{c}'} \quad \mathbf{I}_{3\times3} \quad \mathbf{I}_{3\times3} \quad \mathbf{I}_{3\times3}\right\}$; $\mathrm{diag}\{\bullet\}$ is a block diagonal matrix; $\mathbf{I}_{3\times3}$ is an identity matrix of order three.

The covariance matrix is directly related to the error states in Kalman filter. When the error states change, the covariance matrix needs to be transformed simultaneously

$$\begin{aligned} \mathbf{P}^{\mathrm{c}'}(\mathrm{t}) &= \mathbf{E}\{[\tilde{\mathbf{X}}^{\mathrm{c}'}(\mathrm{t}) - \mathbf{X}^{\mathrm{c}'}(\mathrm{t})][(\mathbf{X}^{\mathrm{c}'}(\mathrm{t}) - \mathbf{X}^{\mathrm{c}'}(\mathrm{t})]^{\mathrm{T}}\} \\ &= \boldsymbol{\Phi} \mathbf{P}^{\mathrm{c}}(\mathrm{t}) \boldsymbol{\Phi}^{\mathrm{T}} \end{aligned} \tag{38}$$

where $\mathbf{P}^{\mathrm{c}}$ is the covariance matrix in the c-frame; $\mathbf{P}^{\mathrm{c}'}$ is the covariance matrix in the c'-frame; Equations (37) and (38) show the mathematical process of transformation the state variable and covariance matrix when the carrier enters the polar regions. The flow of the proposed algorithm is shown below. When the carrier leaves the polar regions, the inverse process of (37) and (38) can be obtained

$$\mathbf{X}^{\mathrm{c}} = \boldsymbol{\Phi}^{-1} \mathbf{X}^{\mathrm{c}'} \tag{39}$$

$$\mathbf{P}^{\mathrm{c}}(\mathrm{t}) = \boldsymbol{\Phi}^{-1} \mathbf{P}^{\mathrm{c}'}(\mathrm{t}) \boldsymbol{\Phi}^{-\mathrm{T}} \tag{40}$$

Algorithm 1 State Transformation for INS/GNSS

Step 1. Initialization: Load initial navigation parameters and receive navigation information from INS and GNSS.

Step 2. Solve the inertial navigation information.

Step 3. Information fusion:

1. Construct the INS/GNSS integrated navigation system dynamic model according to (1).

2. Receive the GNSS measurement information and construct measurement model according to (11).

3. Kalman filter prediction and update.

Step 4. State transformation algorithm:

When latitude reaches 84 degrees

According to the (37) transform state variables, and according to the (38) transform covariance matrix. Continue with Step 2.

else

The transformation process is not required. Continue with Step 2.

end

Step 5. Output navigation results.

IV. Experiment

A. Experiment Setup

In this section, the state transformation algorithm is analyzed based on the navigation data of the Yangtze River. The duration of the experiment is about 3 hours and the sailing distance is about 43 kilometers. The experiment trajectory is shown in Figure 1. The experimental ship carries a set of INS equipment to measure attitude, velocity and position information. There is also a set of GNSS equipment to provide accurate position information, which also provides the measurement information for the integrated INS/GNSS navigation system to complete the data fusion. The performance of the important sensor involved in these devices is shown in Table I.

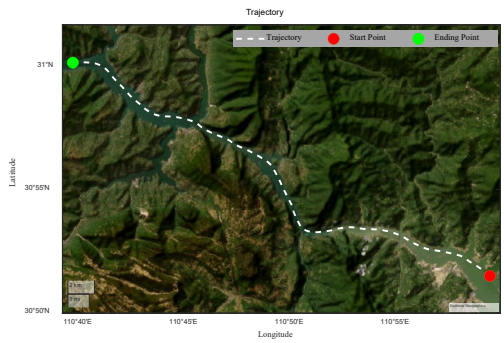

Fig. 1. The navigation trajectory of the experimental ship

TABLE I. THE PERFORMANCE OF SENSOR

Equipment	Performance		
	Indexes	***Parameter***	***Sample Frequency***
INS	Gyro bias stability	<0.02°/h	200HZ
	Accelerometer bias stability	< 50μg	1HZ
GNSS	Positioning accuracy	<5m	1HZ

This experiment focuses on the following aspects: 1. The influence of the proposed algorithm on the INS/GNSS integrated navigation system during the navigation coordinate system switching; 2. The effect of the proposed algorithm on INS/GNSS integrated navigation system in open loop mode and closed loop mode of Kalman filter; It should be noted that the polar navigation data cannot be taken due to limited experimental conditions, but this paper focuses on the effect of the proposed algorithm at the time of Kalman state variable transformation. The experimental data in this paper can realize coordinate system switching and state variable transformation, which is similar to the process of state transformation when entering and leaving the polar regions.

B. Experimental data analysis

Since the INS/GNSS integrated navigation system using the geographic coordinate system as the navigation coordinate system performs well in the middle and low latitudes, the navigation results of it are used as reference result to test the effectiveness of the proposed algorithm. In this experiment, the navigation coordinate system of the INS/GNSS integrated navigation system is switched from the geographic coordinate system to the transversal geographic coordinate system, and the Kalman filter state is transformed concurrently, which is similar to the switching process of the INS/GNSS integrated navigation system when entering the polar region.

In this experiment, the navigation results are smoothed in the unit of 100 seconds. Moreover, the mean and standard deviation of the errors in each unit are calculated with the reference results of INS/GNSS integrated navigation. Finally, the mean curve with the error bar is drawn to reflect the errors and fluctuations of the system. In the closed loop mode, the influence of the state transformation algorithm on the attitude, velocity and position of the system is shown in Figure 2, Figure 3 and Figure 4 respectively

As shown in Figure 2, after the navigation coordinate system is switched, the error mean without state transformation rapidly increases. The pitch error, roll error and yaw error increase to 3.9033″ , 1.1560″ and 112.8687″ respectively. In particular, the navigation yaw error fluctuates greatly, and the standard deviation is up to 20.4524″ . After processing by the state transformation algorithm, the pitch error, roll error and yaw error only increase to 1.3203″ , 0.2621″ and 9.6581″ respectively. Thus, it is obvious that the algorithm proposed in this paper is effective. It is worth mentioning that the roll error shows a divergence trend after a period of time, which may be due to the convergence error of the Kalman filter. Similarly, as can be seen from Figure 3 and Figure 4, both velocity and position fluctuate for a short time after switching. After the state transformation, the fluctuation degree of the system and the error is greatly reduced. Table Ⅱ shows the maximum of the error mean and standard deviation over the six unit time period after the switching. Through these data, it can be clearly seen that the state transformation algorithm can improve the stability of the system and reduce the error when the state variables are transformed.

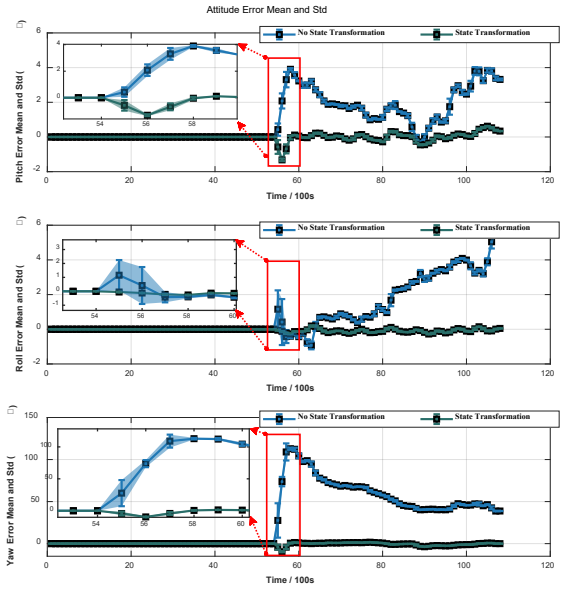

Fig. 2. Attitude error mean and standard deviation curve in the closed loop mode

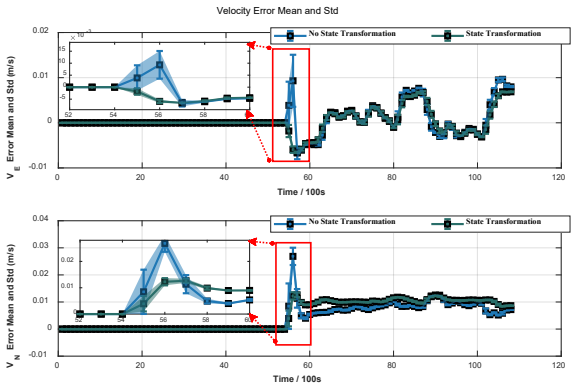

Fig. 3. Velocity error mean and standard deviation curve in the closed loop mode

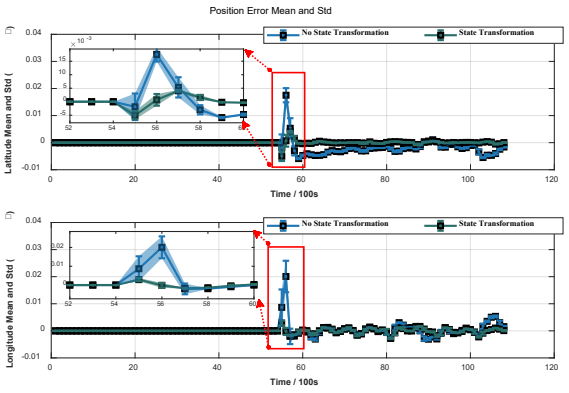

Fig. 4. Position error mean and standard deviation curve in the closed loop mode

Figure 5, Figure 6, and Figure 7 are error mean curves with error bars for attitude, velocity, and position in open loop mode. As can be seen from the figures, in a short time after the switching time, there is a great fluctuation situation, and even a brief overshoot phenomenon. It shows that the Kalman filter working in open loop mode is more sensitive to the state transformation and exhibits more intense fluctuation. Table Ⅱ shows the maximum of the error mean and standard deviation in the six unit time after switching. It can be seen that the errors are greatly and violently increased, compared with the closed loop mode, and the discontinuity of the filter is more obvious. After the state transformation, the error is greatly reduced, the system fluctuation is reduced, and there is no overshoot phenomenon. The data shows that in open loop mode, the state variables transformation has a stronger impact on the system, and the state transformation algorithm is essential.

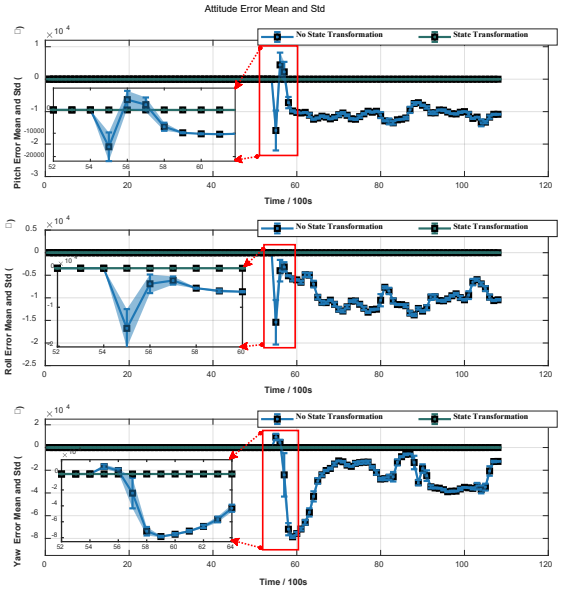

Fig. 5. Attitude error mean and standard deviation curve in the open loop mode

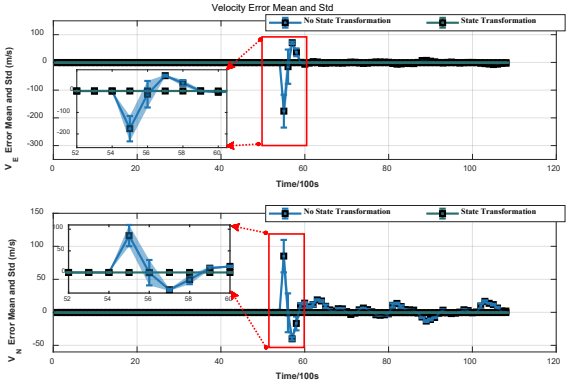

Fig. 6. Velocity error mean and standard deviation curve in the open loop mode

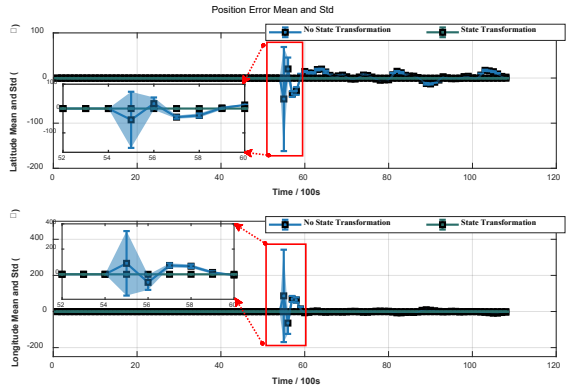

Fig. 7. Position error mean and standard deviation curve in the open loop mod

TABLE II. THE MAXIMUM ERROR MEAN AND STANDARD DEVIATION WITHIN SIX UNITS OF TIME

State error		**No State Transformation**				**State Transformation**			
		Open loop model		***Closed loop model***		***Open loop model***		***Closed loop model***	
		Mean	***Std***	***Mean***	***Std***	***Mean***	***Std***	***Mean***	***Std***
Attitude Error	Pitch	15811.9756″	6146.0738″	3.9033″	0.4443″	3.7055″	0.9965″	1.3203″	0.3972″
	Roll	15407.0309″	4932.4137″	1.1560″	1.3253″	2.1306″	0.2955″	0.2621″	0.0634″
	Yaw	78592.1534″	19113.680″	112.868″	20.452″	24.6589″	7.6335″	9.6581″	2.9851″
Velocity Error	V_E	175.3938 m/s	61.7826 m/s	0.0093 m/s	0.0058 m/s	0.0110 m/s	0.0019 m/s	0.0065 m/s	0.0014 m/s
	V_N	85.3275 m/s	29.4065 m/s	0.0269 m/s	0.0084 m/s	0.0536 m/s	0.0093 m/s	0.0126 m/s	0.0029 m/s
Position Error	Latitude	46.3269″	115.3131″	0.0175″	0.0049″	0.0131″	0.0060″	0.0050″	0.0022″
	Longitude	86.9385″	255.9201″	0.0201″	0.0066″	0.0053″	0.0022″	0.0029″	0.0013″

V. CONCLUSION

By constructing the state variables relationship between the geographic coordinate system and the transversal geographic coordinate system, this paper proposes the state variable transformation algorithm to realize the smooth switching between different coordinate systems, solve the problem of state discontinuity during the switching process, and improve system stability. In different Kalman filter modes, the open loop mode will cause more serious fluctuations, which leads to overshoot and bigger convergence error than the closed loop mode when the state variable is transformed. Thus, the open loop mode is more sensitive to state variables transformation and more susceptible to influence. Although the influence is less in closed loop mode compared with open loop model, the filter discontinuity still exists. Therefore, the state variable transformation algorithm is essential when the Kalman state variables change.

The experiment simulates the process of the integrated navigation system entering the polar region, and the experiment also shows that the state variable transformation can solve the discontinuity problem caused by Kalman filter switching coordinate system , which provides a solution for the global applicability of INS/GNSS integrated navigation. In fact, the algorithm proposed in this paper provides a thought to guarantee the stability of Kalman filters when the Kalman state variables change. Further, this idea can be applied to other Kalman filters to make the system run more stably once the state variables changes.

REFERENCES

[1] H. Xiong, Z. Mai, J. Tang and F. He, "Robust GPS/INS/DVL navigation and positioning method using adaptive federated strong tracking filter based on weighted least square principle," in *IEEE Access*, vol. 7, pp. 26168-26178, 2019.

[2] X. Mu, B. He, S. Wu, X. Zhang, Y. Song, and T. Yan, "A practical INS/GPS/DVL/PS integrated navigation algorithm and its application on Autonomous Underwater Vehicle," *Applied Ocean Research*, vol. 106, p. 102441, Jan. 2021.

[3] S. Taghizadeh and R. Safabakhsh, "An integrated INS/GNSS system with an attention-based hierarchical LSTM during GNSS outage," *GPS Solutions*, vol. 27, no. 71, p. 2, Jan. 2023..

[4] R. Sieradzki and J. Paziewski, "Towards a reliable ionospheric polar patch climatology with ground-based GNSS," *IEEE Transactions on Geoscience and Remote Sensing*, vol. 60, pp. 1–14, Jan. 2022.

[5] C. Hide, T. Moore, and M. Smith, "Adaptive kalman filtering for low-cost INS/GPS," *Journal of Navigation*, pp. 143–152, Jan. 2003.

[6] S. Nassar, "Improving the inertial navigation system (INS) error model for INS and INS/DGPS applications," Jan. 2003.

[7] Q. Fu, Q. Zhou, G. Yan, S. Li, and F. Wu, "Unified All-Earth navigation mechanization and virtual polar region technology," *IEEE Transactions on Instrumentation and Measurement*, pp. 1–11, Jan. 2021.

[8] Y. Yao, X. Xu, Y. Li, Y. Liu, J. Sun, and J. Tong, "Transverse navigation under the ellipsoidal earth model and its performance in both polar and non-polar areas," *The Journal of Navigation*, pp. 335–352, Mar. 2016.

[9] Y. Wu, C. He, and G. Liu, "On inertial navigation and attitude initialization in polar areas," *Satellite Navigation*, Dec. 2020.

[10] L. Zhao, M. Wu, J. Ding, and Y. Kang, "A joint dual-frequency GNSS/SINS deep-coupled navigation system for polar navigation," *Applied Sciences*, vol. 8, no. 11, p. 2322, Nov. 2018.

[11] Y. Ben, W. Cui, and Q. Li, "An improved damping method for grid inertial navigation system in polar region," *IEEE Transactions on Instrumentation and Measurement*, vol. 71, pp. 1–13, Jan. 2022.

[12] Y. Zhang, H. Luo, X. Yu, G. Wei, C. Gao, and L. Wang, "Covariance matrix transformation method in all-earth integrated navigation considering coordinate frame conversion," *Measurement Science and Technology*, p. 065101, Jun. 2022.

[13] Goshen-Meskin, Drora, and Itzhack Y. Bar-Itzhack. "Unified approach to inertial navigation system error modeling." *Journal of Guidance, Control, and Dynamics*, vol. 15, no. 3, pp. 648-653, 1992,

[14] I. Y. Bar-Itzhack and D. Goshen-Meskin, "Identity between INS position and velocity error equations in the true frame," *Journal of Guidance, Control, and Dynamics*, vol. 11, no. 6, pp. 590–592, Nov. 1988.

[15] K. G. Blankinship, "A general theory for inertial navigator error modeling," in *2008 IEEE/ION Position, Location and Navigation Symposium*, Monterey, CA, USA, Jan. 2008.

[16] I. Y. Bar-Itzhack and N. Berman, "Control theoretic approach to inertial navigation systems," in *Guidance, Navigation and Control Conference*, Monterey,CA,U.S.A., Aug. 1987.

[17] E.-H. Shin, "Estimation techniques for low-cost inertial navigation," Jan. 2005.

[18] D. Benson, "A comparison of two approaches to pure-inertial and doppler-inertial error analysis," *IEEE Transactions on Aerospace and Electronic Systems*, pp. 447–455, Jul. 1975,.